Simplicity versus accuracy trade-off in estimating seismic fragility of existing reinforced concrete buildings

Roberto Gentile[1,2], Carmine Galasso[2,3]

[1] Department of Civil, Environmental and Geomatic Engineering, University College London, London, United Kingdom
[2] Institute for Risk and Disaster Reduction, University College London, London, United Kingdom
[3] Scuola Universitaria Superiore (IUSS) Pavia, Pavia, Italy

Correspondence to: Roberto Gentile (r.gentile@ucl.ac.uk)

Abstract. This paper investigates the trade-off between simplicity (modelling effort and computational time) and result accuracy in seismic fragility analysis of reinforced concrete (RC) frames. For many applications, simplified methods focusing on "archetype" structural models are often the state-of-practice. These simplified approaches may provide a rapid-yet-accurate estimation of seismic fragility, requiring a relatively small amount of input data and computational resources. However, such approaches often fail to capture specific structural deficiencies and/or failure mechanisms that might significantly affect the final assessment outcomes (e.g. shear failure in beam-column joints, in-plane and out-of-plane failure of infill walls, among others). To overcome these shortcomings, the alternative response analysis methods considered in this paper are all characterised by 1) a mechanics-based approach; 2) the explicit consideration of record-to-record variability in modelling seismic input/demands. Specifically, this paper compares three different seismic response analysis approaches, each characterized by a different refinement: 1) low refinement - non-linear static analysis (either analytical SLaMA or pushover analysis), coupled with the capacity spectrum method; 2) medium refinement - non-linear time-history analysis of equivalent single degree of freedom (SDoF) systems calibrated based on either the SLaMA-based or the pushover-based force-displacement curves; 3) high refinement - non-linear time-history analysis of multi-degree of freedom (MDoF) numerical models. In all cases, fragility curves are derived through a cloud-based approach employing unscaled real (i.e. recorded) ground motions. 14 four- or eight-storey RC frames showing different plastic mechanisms and distribution of the infills are analysed using each method. The results show that non-linear time-history analysis of equivalent SDoF systems is not substantially superior with respect to a non-linear static analysis coupled with the capacity spectrum method. The estimated median fragility (for different damage states) of the simplified methods generally falls within ±20% (generally as an under-estimation) of the corresponding estimates from the MDoF non-linear time-history analysis, with slightly-higher errors for the uniformly-infilled frames. In this latter cases, such error range increases up to ±32%. The fragility dispersion is generally over-estimated up to 30%. Although such bias levels are generally non-negligible, their rigorous characterisation can potentially guide an analyst to select/use a specific fragility derivation approach, depending on their needs and context, or to calibrate appropriate correction factors for the more simplified methods.

1. Introduction and motivation

Earthquake-induced direct and indirect losses tend to be high in highly-populated earthquake-prone areas, especially in countries where most of the existing buildings and infrastructure is designed/built according to pre-seismic codes (if any). Therefore, there is a dire need to develop holistic strategies for mitigating and managing seismic risk, which first involves risk understanding and quantification. Various end users/stakeholders have different needs on this matter (Figure 1): private owners likely need a detailed assessment focused on individual buildings or small portfolios, while government agencies or (re)insurance companies might look at large portfolios tolerating a lower refinement level and accepting higher uncertainties. In this paper, guidance is provided for selecting suitable seismic fragility analysis approaches to fulfil such needs. Seismic fragility is defined as the likelihood of various damage levels as a function of a hazard intensity measure (IM). Special focus is given to reinforced concrete (RC) frames, which usually represent a large share for both residential and commercial building occupancies among construction types built from 1960s onwards in several counties around the world (and especially in Europe).

This study is part of a larger research project involving different refinements for 1) an exposure module, in which various building-level input data can be supplemented with structure-specific information based on simulated design; 2) a loss estimation module, spanning from the benchmark component-level approach proposed in the Federal Emergency Management Agency (FEMA) P-58 [1] guidelines and the Resilience-based Earthquake Design Initiative (REDi) rating [2] to a simplified building-level damage-to-loss approach; 3) multi-criteria decision making for optimal retrofit selection (e.g. [3]), combined with soft measures such as risk transfer (insurance) and/or tax rebates.

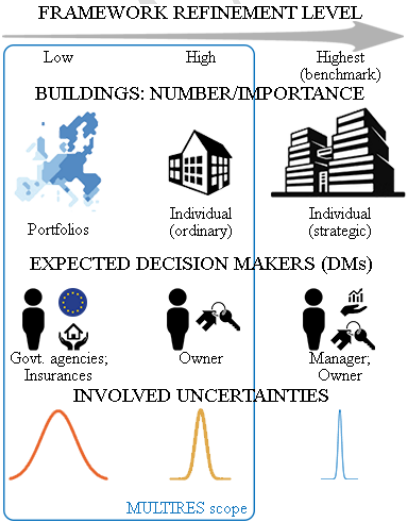

Figure 1 Expected needs of different decision makers.

Non-linear time-history analysis (NLTHA) arguably represents the most advanced procedure for seismic fragility analysis. Yet, it requires a detailed characterisation/modelling of both the structure under investigation and the site-specific hazard

profile (and consequent seismic input modelling/selection), relatively higher computational time/effort, and very specific skills for its implementation/results interpretation. Such a detailed approach is deemed appropriate for individual high-importance buildings (e.g. hospitals, schools) but may result overcomplicated, for instance, for assessing individual ordinary (e.g. residential) buildings. Similarly, such level of detail is not always feasible, or even necessary, for example, in applications dealing with large building portfolios. In the latter case, empirical or simplified numerical methods are often the state-of-practice (e.g. [4,5]). Indeed, these applications typically focus on building classes, often coupled with limited exposure information, which is not compatible with the level of detail and computing required by NLTHA.

Building classes are usually defined as groups of buildings sharing the same materials, lateral-resisting system, height range, and construction age, among other features. Each building class of interest should be fully characterised considering both the within-building and building-to-building variabilities. The former is caused by the uncertainty in the building properties, model, and analysis method; the latter is instead due to the different buildings included in a given building class. Modelling such a building-to-building variability may require substantial knowledge of the building stock under investigation and significant computational resources, for instance, in the case of simulation-based seismic risk assessment. To overcome this, a building class is often represented through a single "archetype" building model, neglecting the variabilities introduced above. Alternatively, a simplified characterisation of building-to-building variability is provided by selecting an adequate number of sample buildings in the class. It is worth mentioning that computationally-cheap methods based on surrogate modelling are generally available to explicitly simulate such a variability (e.g. [6]). In some cases, it is also accepted (e.g. [7]) to use reduced-order models and simplified response analysis methods, often adopting design response spectra (i.e. neglecting record-to-record variability). These simplified approaches may provide a rapid estimation of seismic fragility, requiring a relatively small amount of input data and computational resources. However, current approaches do not capture specific structural deficiencies and/or failure mechanisms that might significantly affect the final assessment outcomes (e.g. plan asymmetry-driven torsional effects, shear failure in beam-column joints, in-plane and out-of-plane failure of infill walls, among others).

For both building-portfolio and building-specific applications, simulated design is generally used to reasonably "guess" unavailable information (e.g. in terms of structural detailing and material properties). However, simulated design can increase the involved epistemic uncertainties, for example, due to the specific knowledge/experience of the analyst with relevant design practices.

It is acknowledged that the combination of adopted models and response analysis methods may bias the performance-assessment results, together with an inaccurate representation of the uncertainties involved [7]. Therefore, a detailed characterisation of such a bias is crucial to guide analysts and, ultimately, develop more informed risk models. This paper aims to analyse such bias in the context of seismic fragility analysis of RC buildings. This study's scope ranges from simplified methods appropriate for building-portfolio analyses to higher-refinement methods suitable for individual ordinary buildings. Higher-refinement methods (e.g. 3D NLTHA of finite element models) related to strategic buildings are outside the scope of this paper. The considered alternative analysis methods involve both non-linear static and dynamic analysis. The considered approaches share some key features: 1) they are mechanics-based; 2) they explicitly consider record-to-record variability in

representing seismic input/demands. Concerning fragility analysis, the following analysis types (Table 1) are considered, from low to high analysis refinement:

1) Simple Lateral Mechanism Analysis (SLaMA) [8–12], which is an analytical version of pushover analysis, combined with the capacity spectrum method (CSM) [13];
2) pushover analysis using computer software (hereafter simply referred to as pushover), combined with the CSM;
3) NLTHA of single-degree-of-freedom (SDoF) systems characterised according to the SLaMA-based force-displacement curve;
4) NLTHA of SDoF systems characterised according to the pushover-based force-displacement curve;
5) NLTHA of an advanced lumped-plasticity 2D MDoF numerical model. It is worth mentioning that MDoF herein refers to a structural model explicitly considering each structural member, as opposed, for instance, to a reduced order model [e.g. 14].

In all cases, fragility curves are derived through a cloud-based approach [15] employing unscaled real (i.e. recorded) ground motions. The relative accuracy of the different analysis types is demonstrated for 14 RC frame buildings, characterised by different height levels (four or eight storeys), plastic mechanisms (global or local), configuration of the infill panels (bare frame, uniformly-infilled frame, pilotis frame). Considering the results from case 5) as a benchmark, critical discussion of the error trends is provided, along with guidance to select the analysis method most consistent with the chosen trade-off between accuracy and simplicity.

Table 1 Adopted seismic response analysis methods

Method	Refinement	Description
CSM-SLaMA	Low	CSM; SLaMA-based force-displacement curve;
CSM-PO	Low	CSM; Pushover-based force-displacement curve;
TH-SDoF-SLaMA	Medium	SDoF time-history; SLaMA-based force-displacement curve;
TH-SDoF-PO	Medium	SDoF time-history; pushover-based force-displacement curve;
TH-MDoF	High/Benchmark	MDoF time-history analysis

2. Methodology

2.1. Seismic response analysis

Regardless of the selected refinement level of the analysis, the seismic response of the analysed structure(s) is represented by a cloud of points in the engineering demand parameter (EDP) vs IM space. The maximum inter-story drift is the selected EDP; it is a convenient proxy highly correlated with (non)structural damage and repair costs. For all the case studies, the selected IM is defined as the geometric mean ($AvgSA$) of the pseudo-spectral acceleration in a structure-specific range of periods depending on the first-mode periods of the case studies (see Section 3.2). This ensures increased efficiency and (relative) sufficiency in estimating a given EDP employing a scalar IM [16,17].

For the application in this work, a set made of 150 unscaled natural (i.e. recorded) ground motions is selected from the SIMBAD database, “Selected Input Motions for displacement-Based Assessment and Design” [18]. As in [19], the 3-

component 467 records in the database are ranked according to their PGA values (by using the geometric mean of the two horizontal components) and then keeping the component with the largest PGA value. The first 150 records are arbitrarily selected; hazard-consistent site-specific record selection is outside the study's scope, especially considering the cloud-based approach for fragility/vulnerability derivation. According to the proposed framework, the resulting EDPs for this suite of ground motions can be computed using increasing refinement methods (Table 1).

Non-linear time-history analyses (*TH-MDoF*), representing the benchmark refinement level, are carried out for advanced 2D lumped-plasticity numerical models (Figure 2) defined using the finite element software Ruaumoko [20]. Mono-dimensional Giberson elements [21] are adopted for the RC members. The beams end sections are characterised by a tri-linear moment-curvature relationship, in addition to the equivalent plastic hinge length [22]. The potential flange effect due to the interaction with the RC slab is accounted for with a 30% increase in the beams' negative moment capacity. Columns are characterised by the axial load-moment interaction diagram and plastic hinge length. Other failure mechanisms (i.e. flexure, bar buckling, lap-splice failure, shear) are evaluated, considering that the weakest link will govern the member ultimate strength and deformation.

The modified Takeda hysteresis [23] is adopted for beams and columns. For the beams, the unloading and reloading stiffness factors are respectively equal to 0.3 and 0.5, while the columns have a thinner loop (the factors are respectively equal to 0.5 and 0). The adjacent beams and columns' rigid ends are connected with non-linear lumped springs modelling beam-column joint panels. Their non-linear behaviour is set consistently with the equivalent column moment-joint drift relationships [9]. The Modified Sina model [23] is adopted for the beam-column joints, thus considering their pinching behaviour. The unloading/reloading stiffness factors are equal to 0.5 and 0, while pinching moment (corresponding to zero deformation) is equal to 25% of the strength. Within-cycle strength degradation of beams, columns and joint panels is set such that a negative stiffness branch in their backbone curves starts from their ultimate capacity and ends (with zero residual strength) at twice the ultimate capacity. The cyclic degradation is set such that strength reduces by 5% at the first plastic excursion (i.e. the response "leaves" the backbone). Such reduction exponentially decreases as the number of plastic excursions increases.

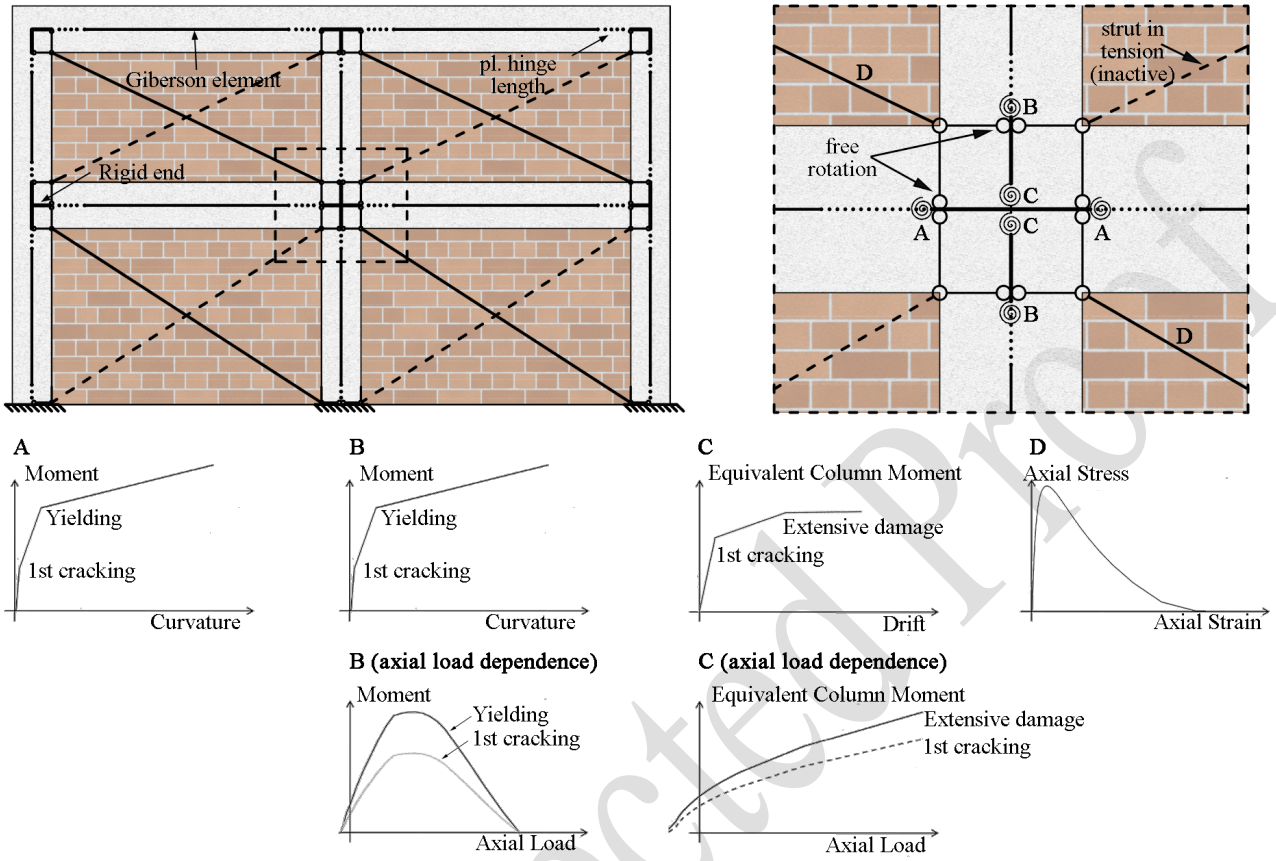

Figure 2 Numerical modelling strategy (modified after [10]**).**

Infill panels are modelled using a single equivalent strut approach. However, the pinned ends of each strut are connected to the beam and column interfaces with the joint panels through two rigid arms (one horizontal, one vertical) able to sustain axial load only. This allows transferring the vertical and horizontal component of the strut's axial load through shear demand for the beam and the column, respectively. The Crisafulli hysteresis is adopted [24], which embeds the within-cycle strength degradation. No cyclic degradation is considered for the infills, implicitly assuming that within-cycle degradation would dominate such members' behaviour.

P-Delta effects due to second-order overturning moments are considered in the analyses. A tangent stiffness-proportional damping equal to 5% of the critical one is adopted for all the vibration modes. Fully fixed boundary conditions are considered at the base, and floor diaphragms are modelled as rigid in their plane. The selected EDP is directly extracted from the *TH-MDoF* analysis results.

In the low-refinement level, the CSM is applied using the suite of real records described above. The formulations provided in [25] are used to calculate the effective mass and the equivalent viscous damping, which is considered the same for both bare and infilled frames. There are two options to derive the structure's force-displacement curve, needed as input for the CSM. The first option is to conduct a Ruaumoko-based pushover analysis adopting the same numerical model described above (*CSM-*

PO). The final capacity curve is expressed in terms of the displacement calculated at the effective height [25], to represent an equivalent SDoF system.

Alternatively, SLaMA can be used to calculate the force-displacement curve (*CSM-SLaMA*). This analytical tool allows one to derive both the expected plastic mechanism and the capacity curve of RC frame, wall and dual-system buildings by using a "by-hand" procedure (i.e. using an electronic spreadsheet). This allows, in turn, the identification of potential structural weaknesses in the lateral-resisting mechanism and to test the reliability of numerical computer models in capturing the most probable behaviour of a structure. Each beam and column in the system is characterised considering many possible failure mechanisms (i.e. flexure, bar buckling, lap-splice failure, shear), considering that the weakest link will govern the overall structural behaviour.

It is worth mentioning that using a real spectrum (i.e. derived from actual ground-motion records) for the CSM, as opposed to an analytically-defined code-based spectrum, may lead to multiple performance points. Based on ongoing work by the authors [26], in such circumstance, the performance point with the smallest displacement is arbitrarily selected among those. After the performance point displacement is calculated for each ground motion, a displacement shape is adopted to calculate the corresponding inter-storey drift. The displacement shapes provided in [9] are adopted in the *CSM-SLaMA* case, while the displacement profile is extracted from the pushover analysis in the *CSM-PO*.

The medium refinement level in the framework involves a set of time-history analyses on an equivalent SDoF model of the structure. The backbone response of the SDoF is calibrated consistently to the non-linear force-displacement curve of the structure, which can be derived both according to SLaMA (*TH-SDoF-SLaMA*) or a pushover analysis (*TH-SDoF-PO*). Generally, the hysteresis rules should be specifically calibrated for each analysed case study. However, the estimation of peak-response EDPs (such as the maximum inter-storey drift; herein selected) is relatively insensitive to the hysteresis parameters [27,28]. Contrarily, residual displacements, not adopted herein as demand parameters, are highly sensitive to the fine-tuning of the hysteresis [27,28].

For the application in this paper, it is chosen to use the modified Takeda hysteresis considering different parameters depending to the expected plastic mechanism of the analysed structure (calculated based on SLaMA or pushover analysis). For global plastic mechanisms, mainly governed by the beams, the unloading and reloading stiffness factors are respectively equal to 0.3 and 0.5 (which are appropriate hysteresis parameters for the beams [25]). For soft-storey mechanisms, those factors are respectively equal to 0.5 and 0 (which are appropriate hysteresis parameters for the columns [25]). The maximum inter-storey drift for each ground motion is calculated based on the registered maximum displacement, and the displacement shapes described above, similarly to the *CSM-SLaMA*/*CSM-PO* cases.

2.2. Fragility estimation

For this study, building-level fragility relationships are calculated for four structure-specific damage state (DSs): slight, moderate, extensive and complete damage. Those DSs are defined according to HAZUS, HAZard United States [4], and

quantified using the non-linear analyses results. This implicitly means that a non-linear static analysis (SLaMA or pushover) is needed regardless of the selected refinement level since this allows such a calibration.

The cloud of points resulting from the analyses is partitioned in two subsets: the "collapse (C)" and the "non-collapse (NoC)" cases. For the *TH-MDoF*, collapse corresponds to the dynamic instability of the analysis, likely caused by a plastic mechanism, or the exceedance of a conventional 10% drift threshold. It is worth mentioning that using numerical dynamic instability as a proxy for the full collapse of structures can be considered as questionable, given that it is reliant on the capability of the modelling strategy and numerical integration algorithm to faithfully reproduce the progressive collapse of structures [29]. Nonetheless, this collapse criterion is quite popular in the literature (e.g. [30]), both for SDoF and MDoF studies. On the other hand, the 10% drift threshold can be interpreted as a particularly-conservative criterion for collapse, for example, according to [30].

The *TH-SDoF* are considerably-less affected by the dynamic instability due to the simplicity of the numerical model. For such analysis method and the CSM-based one, the displacement threshold defining the conventional collapse is defined consistently with the P-Delta instability (i.e. the second-order overturning moment equates the first-order one). According to this particularly-conservative choice, the collapse drift is calculated based on a simplified equilibrium.

Eq. 1 describes the derivation of the fragility functions, where $P(EDP \geq EDP_{DS}|IM, NoC)$ is the conditional probability that the EDP threshold (for a given DS) is exceeded given that collapse does not occur (for the given IM level), and $P(C|IM)$ is the probability of collapse at the same IM level. It is implicitly assumed that the EDP threshold (EDP_{DS}) is exceeded for collapse cases, i.e. $P(EDP \geq EDP_{DS}|IM, C) = 1$.

$$P(EDP \geq EDP_{DS}|IM) = P(EDP \geq EDP_{DS}|IM, NoC)(1 - P(C|IM)) + P(C|IM) \quad (1)$$

The linear least square method is applied on the "NoC" EDP-IM pairs to derive the commonly-used power-law probabilistic seismic demand model $EDP = aIM^b$, where a and b are the parameters of the regression. This allows defining a lognormal cumulative distribution function (CDF) representing $P(EDP \geq EDP_{DS}|IM, NoC)$ for a given DS. The probability of collapse $P(C|IM)$ is fitted with a logistic regression, which is appropriate for cases in which the response variable is binary ("collapsed" or "non-collapsed"). As in [6], the final result is converted into a lognormal CDF, defined by a median and a logarithmic standard deviation (or simply dispersion).

2.3. Description of the case study frames

The five considered analysis types are carried out for 14 case study RC frames shown in Figure 3. The case studies have four bays and either four or eight storeys. For each geometrical configuration, three different solutions are adopted for the detailing of the RC members, leading to three different expected plastic mechanisms: Beam-Sway (all beams and the base columns yield), Mixed-Sway (combination of joint shear failures with beam and/or column flexure, shear or lap-splice failures) and Column-Sway (soft storey mechanism at ground storey). For each plastic mechanism configuration, both a bare and a uniformly-infilled configuration is considered. Finally, a pilotis configuration (infills missing at the ground floor) is also

considered for the Column-Sway cases. The reader is referred to [10] for details on the design of the case studies, the member detailing of each RC member, the adopted material models, the load analysis and mass properties.

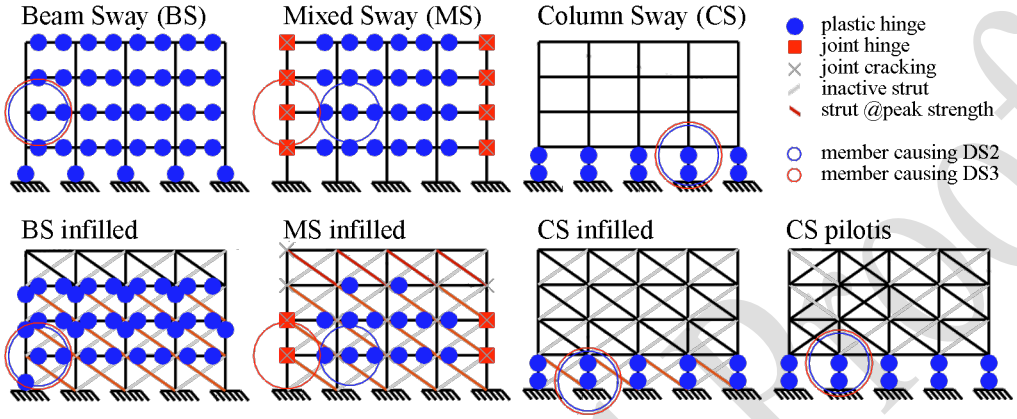

For each case study, there is an 8-storey one with the same plastic mechanism.

Figure 3 Plastic mechanism (DS3) for the analysed case studies [31]**. 8-storey ones are not shown for brevity.**

3. Results and discussion

3.1. Non-linear static analyses

The results of the non-linear static analyses are discussed first, since those are required regardless of the chosen refinement level of the analysis (as mentioned in Section 2.2). A summary of the results for all the case studies is shown in Figure 4, expressed in terms of the displacement at the effective height, obtained interpolating the displacement profile Δ_i at the effective height $H_e = \sum m_i \Delta_i H_i / \sum m_i \Delta_i$, and base shear normalised by the effective weight (the effective mass is $m_e = \sum m_i \Delta_i^2 / \Delta_e$, where m_i is the mass of storey i and Δ_e is the effective height displacement).

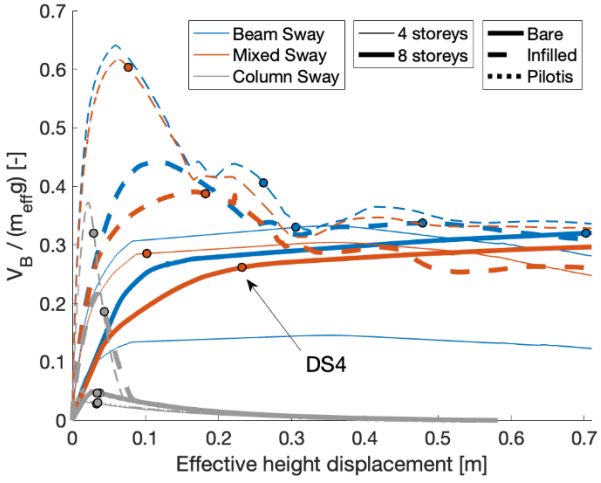

Figure 4 Pushover curves for all the case studies (modified after [31]**).**

As an example, Figure 5a shows the comparison of the pushover- and the SLaMA-based force-displacement curves for the Mixed-Sway, 4-storey bare frame, together with the plastic mechanism developed at DS3 (which is considered as the ultimate limit state, consistently with Eurocode 8 [32]). As discussed in detail in [9,10], there is a particularly good match between the SLaMA and pushover curves at DS3 both in terms of displacement and base shear for all the 4-storey case studies, while a slightly larger error is observed for the 8-storey ones. As expected, a more significant error is observed for the initial stiffness, due to the over-estimation of the yielding base shear. As already demonstrated in [10], SLaMA considerably over-estimates the peak base shear capacity of the uniformly-infilled frames. Figure 5a also shows the quantification of the DS thresholds based on the non-linear analysis results. All the SLaMA curves (typically ending at DS3) are extended up to the P-Delta point, where the second-order overturning moment equates the first-order one. Consistently with Eurocode 8 [32], the DS4 displacement is equal to four-thirds of the DS3 one.

Figure 5b,c show the assumed SDoF capacity curves for the Mixed-Sway, 4-storey bare and 8-storey infilled frames. The pushover-based SDoF curves are obtained by a multi-linear fit of the pushover curve, calculated consistently with the provisions by the Applied Technology Council [33]. The same procedure is used for the SLaMA-based SDoF curves of the uniformly-infilled frames, to consider the post-peak strength degradation appropriately. On the other hand, the SLaMA-based force-displacement curve residual strength for bare frames (typically neglected in SLaMA) is assumed equal to 50% for Beam- and Mixed-Sway cases. 75% strength degradation is considered for the Column-Sway frames, due to the pronounced softening behaviour of the first-storey columns, starting soon after yielding. Finally, a linear behaviour is assumed for the within-cycle degradation, which begins at DS4 and ends at twice such displacement. This assumption for strength degradation in SLaMA leads to significant discrepancies with the pushover curve for Beam- and Mixed-Sway bare frames (this issue is not evident for Column-Sway cases). As discussed in Section 3.2, since such mismatch develops only for very large displacements, it does not jeopardise the fragility results.

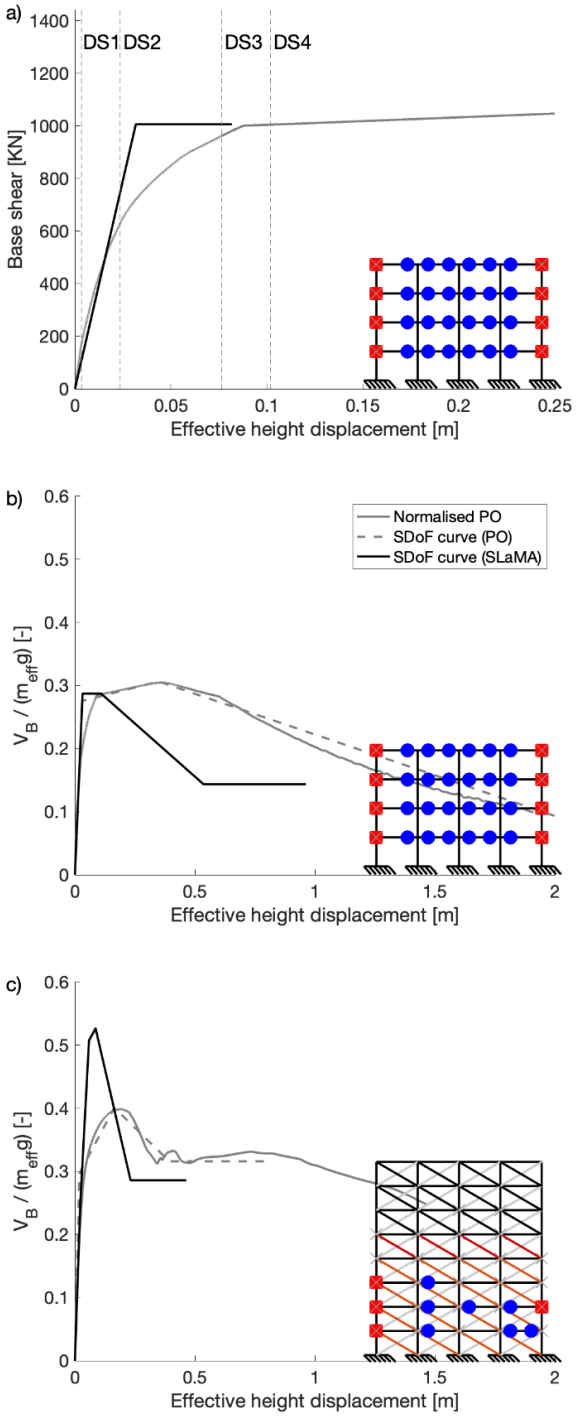

Figure 5 a) Mixed-Sway 4-storey bare frame: pushover curve, SLaMA curve and plastic mechanism at DS3; b,c) assumed curves for SDoF representation [b) 4-storey bare; c) 8-storey infilled].

Table 2 shows the drift-based DS threshold calibrated based on the non-linear static results. Moreover, the table shows some dynamic elastic properties of the case studies. The fundamental period of the 8-storey frames is approximately double with respect to the 4-storey ones. Moreover, the presence of infills reduces the fundamental period by about 50%. The only exception is the pilotis frames, which have a similar period with respect to the bare ones.

The participating mass of the first vibration mode is approximately equal to 85% for the Beam-Sway and Mixed-Sway, 4-storey bare and uniformly-infilled frames (80% for the 8-storey ones), while it is greater than 95% for the Column-Sway cases studies. The analysed structures are, therefore, first-mode dominated, which justifies using simplified response analysis methods.

Table 2 Drift-based DS thresholds [%]. BS: beam sway; MS: mixed sway; CS: column sway; T_1: fundamental period; M_1^* participating mass of the fundamental mode.

	Four storeys							Eight storeys						
	Bare			Uniformly infilled			Pilotis	Bare			Uniformly infilled			Pilotis
	BS	MS	CS	BS	MS	CS	CS	BS	MS	CS	BS	MS	CS	CS
T_1[s]	0.48	0.50	1.06	0.18	0.19	0.22	0.99	0.97	1.02	1.19	0.38	0.38	0.44	0.82
M_1^*[%]	84	83	99	89	88	98	100	81	81	92	82	82	81	99
DS1	0.03	0.03	0.08	0.03	0.03	0.05	0.08	0.14	0.17	0.05	0.02	0.01	0.04	0.06
DS2	0.24	0.19	0.42	0.19	0.19	0.18	0.44	0.34	0.33	0.27	0.18	0.17	0.17	0.31
DS3	2.10	1.32	0.74	2.56	1.31	0.60	0.78	2.91	1.37	0.66	3.17	1.36	0.69	0.73
DS4	2.90	1.76	0.99	3.16	1.74	0.83	1.05	3.92	1.82	0.95	4.39	2.21	1.08	0.99

3.2. Seismic response and fragility analyses

Figure 6a,c show the results of the seismic response analysis for the Mixed-Sway, 4-storey bare and 8-storey infilled frames. Given the high strength and the particularly-stable response behaviour up to high displacements, no collapse is registered for these case studies. However, this is not the case for the Column-Sway frames, which show considerably less strength. Moreover, the first-storey columns of these case studies show a pronounced softening behaviour, which causes a softening response of the whole first storey and, in turn, of the entire structure. In the time-history analyses (medium and high refinement level), this causes instability phenomena due to P-Delta effects, which are clearly more evident for the 8-storey frames.

There is a particularly good match among the clouds across all refinement levels of the framework, as well as for the probabilistic seismic demand models. This confirms the effectiveness of the simplified analysis methods for the considered case studies; which are dominated by their first-mode response. Such a result reflects in the calculated fragility curves. Figure 6b,d qualitatively shows the good match obtained for the DS3 fragility curves across all the considered analysis methods.

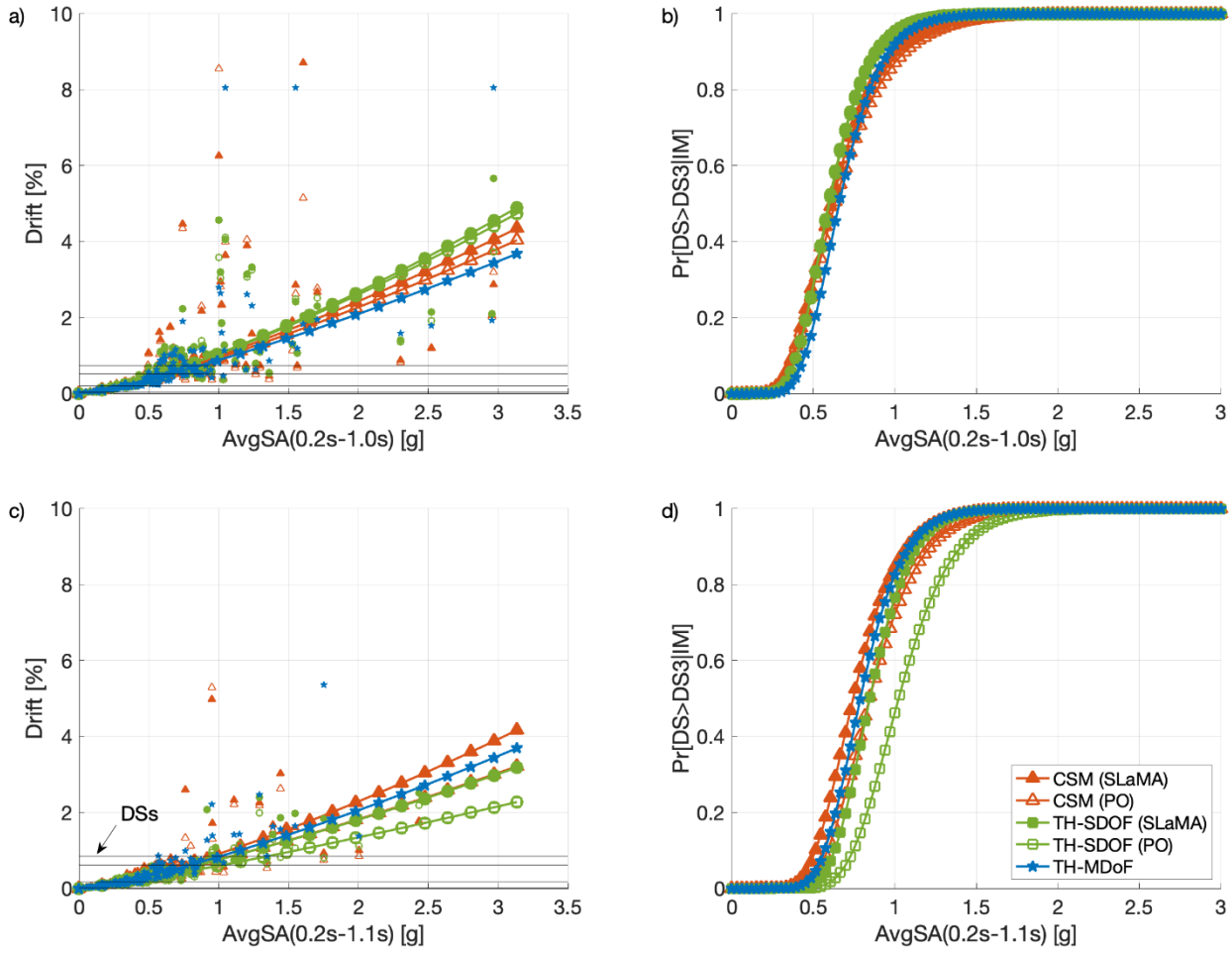

Figure 6 Mixed-Sway frames: seismic response analysis [a) 4-storey bare; c) 8-storey infilled]; DS3 fragility curves [b) 4-storey bare; d) 8-storey infilled].

The discussion of the fragility parameters' overall results mainly focuses on the damage limitation (DS2) and life-safety damage state (DS3). In fact, the results for DS1 and DS4 are consistent with those for DS2 and DS3, respectively. As a measure of the accuracy of the simplified methods, Table 3 shows the "F-ratios" for DS2 and DS3: the ratio of the fragility parameters (median and dispersion) of a given analysis method with respect to the *TH-MDoF* ones. In addition, Figure 7 shows the F-ratios for DS3.

Considering the bare and pilotis frames, the estimated DS3 median fragility of the low- and medium-refinement methods approximately falls within ±20% of *TH-MDoF*, generally leading to conservative estimations (under-estimation), apart from the 8-storey, mixed-sway case. This shows the high accuracy of such analysis methods, despite their inherent simplification. The above error range increases up to ±32% for the uniformly-infilled frames. This is likely linked to the complex evolution

of infilled frames' dynamic behaviour as damage spreads (e.g. elongation of the fundamental period and different distribution of higher modes), which are not adequately captured in the low- and medium-refinement levels of the framework. A similar trend is observed for the DS4 fragility median, with the error bounded within $\pm 20\%$, and only slightly exceeding it for the column-sway, uniformly-infilled case studies.

The low- and medium-refinement methods approximately provide a maximum 20% under-estimation of the DS2 fragility median. The under-estimation is higher (up to 30%) for the column-sway, infilled case studies. As mentioned above, this is likely due to the simplified methods' inability to capture the complex dynamic non-linear behaviour of infilled frames adequately. Although the qualitative error trend for the DS1 median is similar to the DS2 one, the relative errors are higher. However, this is likely affected by the very low DS1 fragility (averaging 0.04g for *TH-MDoF*), and it does not represent a shift from the main error trend.

The fragility dispersion error is more uniform, approximately bounded in the range $\pm 30\%$ for all DSs and case studies, generally leading to an over-estimation. The column-sway case studies show a slightly higher error (up to 45% over-estimation). Such result is likely connected with the collapse estimation, based on both dynamic instability (when appropriate) and the use of a conventional drift threshold. Indeed, a numerical instability is more likely for the *TH-MDoF* method rather than the *TH-SDoF* one. However, this is more-clearly connected with a physical instability (P-Delta driven) for the *TH-SDoF*, while also triggered by local numerical convergence issues for the *TH-MDoF*. For this reason, the collapse probability function based on *TH-MDoF* is sharper, thus leading to fragility curves with smaller dispersion.

An interesting aspect of the results is that the *TH-SDoF* method is not substantially superior with respect to the analytical CSM. For a given characterisation of the capacity curve (SLaMA or pushover), both methods show a similar bias with respect to the *TH-MDoF* for bare and pilotis frames. Slightly-higher differences are observed for the uniformly-infilled case studies. This may be caused by using (in the CSM) the equivalent viscous damping model calibrated for bare frames, which may be inappropriate for infilled frames.

The comparison between the SLaMA- and pushover-based methods, for a given response analysis approach (*CSM* or *TH-SDoF*), shows that for bare and pilotis frames the SLaMA-vs-pushover error on the capacity curve has little-to-no effect on the estimation of fragility median for all DSs. On the other hand, higher errors are observed for the infilled frames (at DS3 only), caused by the propagation of the SLaMA-vs-pushover discrepancy for the peak base shear in the capacity curve, already reported in [10]. However, it is worth mentioning that such error propagation is only significant for the DS3 median fragility of the column-sway, uniformly-infilled frames, causing shifts in the fragility median as high as 35%. Negligible effects are observed for the estimation of the fragility dispersion. This propagation effect is remarkably similar across all DSs, and is overall not deemed to be significant.

Although out of scope for this paper, such errors should be propagated further up to portfolio-level seismic loss estimation, which is usually the final aim of a risk model. As demonstrated by previous studies (e.g. [31,32]), large epistemic uncertainties affect such loss estimations. At least arguably, the highlighted error trends of the simplified response analysis methods with respect to a time-history assessment are likely to have a smaller effect if compared to epistemic uncertainties. For this reason,

the measured error trends are deemed reasonable. Moreover, the calibrated F-ratios can be used to "correct" the fragility predictions obtained by the quick simplified analysis methods, while obtaining a higher accuracy.

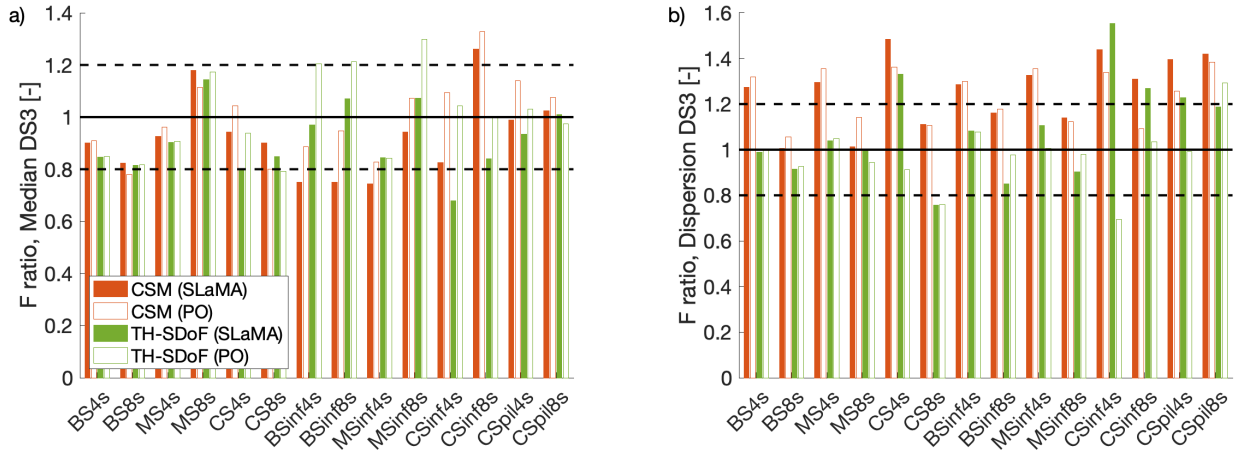

Figure 7 Fragility parameters of the low- and medium-refinement methods as a ratio of the *TH-MDoF* ("F-ratios"): a) DS3 median; b) DS3 dispersion. [BS: Beam-Sway; MS: Mixed-Sway; CS: Column-Sway; 4s: four storeys; 8s: eight storeys; inf: uniformly infilled; pil: pilotis]

Table 3 F-ratios for DS2 and DS3. [SL: SLaMA; PO: pushover; BS: Beam-Sway; MS: Mixed-Sway; CS: Column-Sway; 4s: four storeys; 8s: eight storeys; inf: uniformly infilled; pil: pilotis]

	DS2								DS3							
	CSM(SL)		CSM(PO)		TH-SDoF(SL)		TH-SDoF(PO)		CSM(SL)		CSM(PO)		TH-SDoF(SL)		TH-SDoF(PO)	
	μ	β	μ	β	μ	μ	μ	β	μ	β	μ	β	μ	μ	μ	β
BS4s	0.92	1.27	0.92	1.32	0.91	0.99	0.91	1.00	0.90	1.27	0.91	1.32	0.85	0.99	0.85	1.00
BS8s	1.09	1.01	1.06	1.06	1.08	0.92	1.08	0.93	0.82	1.01	0.78	1.06	0.82	0.92	0.82	0.93
MS4s	0.95	1.29	0.97	1.35	0.95	1.04	0.95	1.05	0.93	1.29	0.96	1.36	0.90	1.04	0.91	1.05
MS8s	1.23	1.00	1.18	1.13	1.21	0.99	1.23	0.93	1.18	1.01	1.11	1.14	1.14	1.00	1.17	0.94
CS4s	0.79	1.41	0.91	1.30	0.79	1.32	0.90	0.86	0.94	1.48	1.04	1.36	0.80	1.33	0.94	0.91
CS8s	0.82	1.08	0.68	1.08	0.82	0.74	0.74	0.74	0.90	1.11	0.80	1.11	0.85	0.76	0.79	0.76
BSinf4s	0.73	1.28	0.76	1.30	0.82	1.08	0.95	1.08	0.75	1.28	0.89	1.30	0.97	1.08	1.20	1.08
BSinf8s	0.86	1.16	0.94	1.18	0.96	0.85	1.03	0.98	0.75	1.16	0.95	1.18	1.07	0.85	1.21	0.98
MSinf4s	0.74	1.33	0.77	1.36	0.84	1.11	0.84	1.01	0.74	1.33	0.83	1.36	0.84	1.11	0.84	1.01
MSinf8s	0.96	1.14	1.04	1.12	1.04	0.90	1.16	0.98	0.94	1.14	1.07	1.12	1.07	0.90	1.30	0.98
CSinf4s	0.70	1.39	0.79	1.33	0.76	1.33	0.79	1.03	0.83	1.44	1.09	1.34	0.68	1.55	1.04	0.70
CSinf8s	0.76	1.29	0.75	1.09	0.71	1.28	0.75	1.34	1.26	1.31	1.33	1.09	0.84	1.27	1.00	1.04
CSpil4s	0.82	1.33	1.01	1.21	0.86	1.17	1.00	0.94	0.99	1.40	1.14	1.26	0.93	1.23	1.03	0.99
CSpil8s	0.92	1.34	0.99	1.29	0.97	1.13	0.93	1.23	1.02	1.42	1.07	1.38	1.01	1.19	0.97	1.29

The results from this study are in good agreement with the findings in [7], although the latter reference discussed various EDPs, highlighting that "*employing static pushover–based approaches introduces non-negligible errors in the assessment that will increase for force/moment quantities or quantities of any kind as more local results (e.g. story drifts or plastic hinge rotations rather than roof drift) are sought*." In particular, it is emphasised that storey shears and overturning moments (not explicitly considered in this study) tend to be consistently underestimated even for simple mid-rise structures, introducing an

unconservative bias when assessing brittle modes of failure. Consistently with the findings from the study presented here, such a bias becomes more significant for taller structures. Reference [7] also highlights that "*most code-like pushover approaches tend to disregard record-to-record variability, offering a single "central" (mean or median, typically unspecified) response estimate for any quantity of interest*". Obviously, this is not acceptable for fragility/vulnerability purposes, and the methods proposed in the present study can help address this issue.

4. Conclusions

This paper provided guidance for selecting suitable seismic fragility analysis methods to fulfil the needs of different end users/stakeholders with regard to seismic risk quantification. Private owners likely need a detailed analysis consisting of single buildings or small portfolios of buildings while government agencies or (re)insurance companies might look at large portfolios tolerating a lower refinement level and accepting higher uncertainties. Particular focus is given to RC frames, which usually represent a high share for both residential and commercial occupancy among construction types built from 1960s onwards.

Three different levels of refinement for the seismic response analysis are considered: 1) low refinement - non-linear static analysis (analytical SLaMA or software-based pushover), coupled with the CSM; 2) medium refinement - non-linear time-history analysis of SDoF systems calibrated based on either the SLaMA or the pushover curve; 3) high refinement - non-linear time-history analysis of MDoF numerical models. All refinement levels are used to assess 14 RC frame buildings, characterised by different height levels (four or eight storeys), plastic mechanisms (Beam-Sway, Mixed-Sway and Column-Sway), configuration of the infill panels (bare frame, uniformly-infilled frame, pilotis frame). The results can be summarised as follows:

- For the bare and pilotis frames, the estimated median fragility of the low- and medium-refinement methods falls within $\pm 20\%$ (generally as an under-estimation) of the corresponding estimates from the MDoF time-history analysis. The above error range increases up to $\pm 32\%$ for the uniformly-infilled frames. This result is valid for al DSs, with a slight increase for DS1;
- The fragility dispersion error is more uniform, approximately bounded in the range $\pm 30\%$ for all DSs and case studies, generally leading to an over-estimation. The column-sway case studies show a slightly higher error (up to 45% over-estimation);
- The time-history analysis of SDoF systems is not substantially superior with respect to a non-linear static analysis coupled with the CSM, regardless of the adopted characterisation of the capacity curve (SLaMA or pushover);
- For a given response analysis approach (CSM or SDoF time-history analysis), for bare and pilotis frames the SLaMA-vs-pushover error on the capacity curve has little-to-no effect on the estimation of fragility median. Higher errors are observed for the DS3 fragility median of the infilled frames, caused by propagating the SLaMA-vs-pushover discrepancy for the peak base shear in the capacity curve. Negligible effects are observed for the estimation of the

fragility dispersion. This propagation effect is remarkably similar across all DSs, and is overall not deemed to be significant;

- Although the bias levels of the simplified methods with respect to the MDoF time-history analyses are generally non-negligible, their rigorous characterisation can potentially guide an analyst to select/use a specific fragility derivation approach, depending on their needs and context, or to calibrate appropriate correction factors for the more simplified methods. Thus, the quick simplified methods may still be adopted to predict seismic fragility, while obtaining a higher accuracy by correcting the resulting predictions.

The low- and medium- refinement analysis methods are deemed to be acceptable for portfolio-level assessments, or for preliminary, more detailed investigations on single assets. In fact, the highlighted error trends with respect to a time-history-based assessment have arguably an effect smaller than the one caused by other epistemic uncertainties involved in applications within an industry context. More in general, fragility estimates obtained via non-linear static methods are satisfactory. Such result is deemed important since pushover-based methods are intuitive and easy to use/computationally inexpensive for engineering practitioners.

Acknowledgements

The authors would like to express their gratitude to two anonymous reviewers that allowed great improvements to the manuscript. This study has received funding from the European Union's Horizon 2020 research and innovation programme under grant agreement No. 843794. (Marie Skłodowska-Curie Research Grants Scheme MSCA-IF-2018: MULTIRES, MULTI-level framework to enhance seismic RESilience of RC buildings) for RG. CG was supported by the project "Dipartimenti di Eccellenza", funded by the Italian Ministry of Education, University and Research at IUSS Pavia.

References

[1] Federal Emergency Management Agency. Seismic Performance Assessment of Buildings. Volume 1 - Methodology. Washington, DC: 2012.

[2] Almuftti I, Willford MR. Resilience-based Earthquake Design Initiative (REDi) for the Next Generation of Buildings. ARUP Report, October 2013: 2013.

[3] Gentile R, Galasso C. Simplified seismic loss assessment for optimal structural retrofit of RC buildings [Open Access]. Earthq Spectra 2020;in press. doi:10.1177/8755293020952441.

[4] Kircher CA, Whitman R V., Holmes WT. HAZUS Earthquake Loss Estimation Methods. Nat Hazards Rev 2006;7:45–59. doi:10.1061/(asce)1527-6988(2006)7:2(45).

[5] Basaglia A, Aprile A, Spacone E, Pilla F. Performance-based Seismic Risk Assessment of Urban Systems. Int J Archit Herit 2018. doi:10.1080/15583058.2018.1503371.

[6] Gentile R, Galasso C. Gaussian process regression for seismic fragility assessment of building portfolios. Struct Saf 2020;87. doi:10.1016/j.strusafe.2020.101980.

[7] Silva V, Akkar S, Baker J, Bazzurro P, Castro JM, Crowley H, et al. Current Challenges and Future Trends in Analytical Fragility and Vulnerability Modeling. Earthq Spectra 2019;35:1927–52. doi:10.1193/042418EQS101O.

[8] New Zealand Society for Earthquake Engineering (NZSEE). The seismic assessment of existing buildings - technical guidelines for engineering assessments. Wellington, New Zealand: 2017.

[9] Gentile R, del Vecchio C, Pampanin S, Raffaele D, Uva G. Refinement and Validation of the Simple Lateral Mechanism Analysis (SLaMA) Procedure for RC Frames [Open Access]. J Earthq Eng 2019. doi:10.1080/13632469.2018.1560377.

[10] Gentile R, Pampanin S, Raffaele D, Uva G. Non-linear analysis of RC masonry-infilled frames using the SLaMA method: part 2—parametric analysis and validation of the procedure [Open Access]. Bull Earthq Eng 2019;17:3305–26. doi:10.1007/s10518-019-00584-6.

[11] Gentile R, Pampanin S, Raffaele D, Uva G. Non-linear analysis of RC masonry-infilled frames using the SLaMA method: part 1—mechanical interpretation of the infill/frame interaction and formulation of the procedure [Open Access]. Bull Earthq Eng 2019;17:3283–304. doi:10.1007/s10518-019-00580-w.

[12] Gentile R, Pampanin S, Raffaele D, Uva G. Analytical seismic assessment of RC dual wall/frame systems using SLaMA: Proposal and validation [Open Access]. Eng Struct 2019;188:493–505. doi:10.1016/j.engstruct.2019.03.029.

[13] Freeman SA. Development and use of capacity spectrum method. 6th U.S. Natl. Conf. Earthq. Engnineering, Seattle: 1998.

[14] Xiong C, Lu X, Guan H, Xu Z. A non-linear computational model for regional seismic simulation of tall buildings. Bull Earthq Eng 2016. doi:10.1007/s10518-016-9880-0.

[15] Jalayer F, Cornell CA. Alternative non-linear demand estimation methods for probability-based seismic assessments. Earthq Eng Struct Dyn 2009;38:951–72. doi:10.1002/eqe.876.

[16] Kohrangi M, Kotha SR, Bazzurro P. Ground-motion models for average spectral acceleration in a period range: Direct and indirect methods. Bull Earthq Eng 2018;16:45–65. doi:10.1007/s10518-017-0216-5.

[17] Minas S, Galasso C. Accounting for spectral shape in simplified fragility analysis of case-study reinforced concrete frames. Soil Dyn Earthq Eng 2019;119:91–103. doi:10.1016/j.soildyn.2018.12.025.

[18] Smerzini C, Galasso C, Iervolino I, Paolucci R. Ground motion record selection based on broadband spectral compatibility. Earthq Spectra 2014;30:1427–48. doi:10.1193/052312EQS197M.

[19] Rossetto T, Gehl P, Minas S, Galasso C, Duffour P, Douglas J, et al. FRACAS: A capacity spectrum approach for seismic fragility assessment including record-to-record variability. Eng Struct 2016;125:337–48. doi:10.1016/j.engstruct.2016.06.043.

[20] Carr AJ. RUAUMOKO2D - The Maori God of Volcanoes and Earthquakes. Inelastic Analysis Finite Element program. Christchurch, New Zealand: 2016.

[21] Sharpe RD. The Seismic Response of Inelastic Structures. Department of Civil Engineering, University of Canterbury, Christchurch, New Zealand., 1976.

[22] Priestley MJN, Calvi GM, Kowalsky MJ. Displacement-based seismic design of structures. IUSS Press, Pavia, Italy; 2007.

[23] Saiidi M, Sozen M. Simple and complex models for non-linear seismic response of reinforced concrete structures. Urbana, Illinois, USA: 1979.

[24] Crisafulli FJ. Seismic behaviour of reinforced concrete structures with masonry infills. University of Canterbury, 1997.

[25] Priestley MJN, Calvi GM, Kowalsky MJ. Direct displacement-based seismic design of structures. Pavia, Italy: IUSS Press; 2007.

[26] Caricati M. Displacement-based assessment con l'impiego di spettri di domanda reali (in Italian). Politechnic University of Bari, 2020.

[27] Kazantzi AK, Vamvatsikos D. The hysteretic energy as a performance measure in analytical studies. Earthq Spectra 2018;34:719–39. doi:10.1193/112816EQS207M.

[28] Priestley M. Myths and fallacies in earthquake engineering - conflicts between design and reality. Bull New Zeal Soc Earthq Eng 1993;26:329–41.

[29] Adam C, Ibarra LF. Seismic collapse assessment. In: Beer M, Kougioumtzoglou IA, Patelli E, Siu- Kui Au I Earthq. Eng. Encycl. vol 3. Springer, Berlin, pp 2729–2752, 2015.

[30] Vamvatsikos D, Cornell CA. Direct estimation of the seismic demand and capacity of MDOF systems through Incremental Dynamic Analysis of an SDOF approximation. J Struct Eng 2005.

[31] Gentile R, Galasso C. Hysteretic energy-based state-dependent fragility for ground motion sequences [Open Access]. Earthq Eng Struct Dyn 2020;in press. doi:10.1002/eqe.3387.

[32] European Committee for Standardisation (CEN). Eurocode 8: Design of structures for earthquake resistance. Part 3: Strengthening and repair of buildings 2005.

[33] ATC 40. Applied Technology Council, Seismic evaluation and retrofit of concrete buildings. Redwood City; 1996.

[34] Silva V, Crowley H, Varum H, Pinho R, Sousa R. Evaluation of analytical methodologies used to derive vulnerability functions. Earthq Eng Struct Dyn 2014. doi:10.1002/eqe.2337.

[35] Silva V. Uncertainty and correlation in seismic vulnerability functions of building classes. Earthq Spectra 2019;35:1515–39. doi:10.1193/013018EQS031M.